Crystallization behavior of a Na_2SO_4–$MgSO_4$ salt mixture and comparison to single salt behavior

N. Lindström*, T. Talreja, K. Linnow and M. Steiger
Department of Chemistry, University of Hamburg,
Inorganic and Applied Chemistry, Hamburg, Germany
* Nadine.Lindstroem@chemie.uni-hamburg.de

Abstract

Crystals growing in confined spaces can generate stress and are a major cause of damage in porous materials. While the behavior of several single salts is well characterized, only few studies have been carried out on the behavior of salt mixtures and, especially, mixtures involving the formation of double salts have not been systematically investigated. Double salts show a complex crystallization behavior and an incongruently soluble salt may have a great damage potential, because a solution supersaturated with one of its single salt compounds is formed during its dissolution. In this study we report on wetting−drying experiments with an equimolar Na_2SO_4–$MgSO_4$ salt mixture. In situ Raman microscopy was used to study the phase transformations during the wetting of the double salts $Na_2Mg(SO_4)_2 \cdot 4H_2O$ (bloedite) and $Na_2Mg(SO_4)_2 \cdot 5H_2O$ (konyaite). Though both salts are incongruently soluble and should form mirabilite upon dissolution, it was found that they behave similar to congruently soluble salts. Most likely, the resulting supersaturation is not sufficient for mirabilite nucleation to occur. Due to the low supersaturation the damage potential of the dissolution of the incongruently soluble double salts bloedite and konyaite is not only much lower than that of sodium sulfate and magnesium sulfate but also in comparison to the incongruently soluble double salt darapskite.

Keywords: sodium sulfate, magnesium sulfate, salt mixtures, bloedite, konyaite

1   Introduction

Crystals growing in confined spaces can generate stress if in contact with their own supersaturated solution and are a major cause of damage in porous materials. The behavior of several single salts that are commonly found in building materials is well characterized. Many studies focused on the behavior of sodium sulfate and magnesium sulfate as these salts were found to be particularly damaging [e.g. 1–8 among others]. However, contamination of building materials with a single salt is uncommon. Usually, the salt systems found are comprised of many different ions. Compared to single salts, the crystallization behavior of salt mixtures is much more complicated. It is not a trivial task to predict, for a given mixture composition, the crystallization sequence, i.e. the nature of the solid phases that crystallize out. Only few experimental studies have been carried out on the crystallization behavior and the damage potential of salt mixtures [e.g. 9,10]. One complicating factor in studies with salt mixtures is that a number of double salts may form in mixed solutions [11], a problem that was tackled in several recent studies [12–14]. These authors studied behavior of Na_2SO_4–$NaNO_3$ and Na_2SO_4–K_2SO_4 salt mixtures including the formation of the incongruently soluble double salts $Na_3NO_3SO_4 \cdot H_2O$ (darapskite) and $K_3Na(SO_4)_2$ (glaserite). The present study reports on experiments on the crystallization behavior of Na_2SO_4–$MgSO_4$ mixtures including the formation of the incongruently soluble double salts $Na_2Mg(SO_4)_2 \cdot 4H_2O$ (bloedite, also known as astrakanite) and $Na_2Mg(SO_4)_2 \cdot 5H_2O$ (konyaite).

Most double salts found in building materials are incongruently soluble which means that they precipitate from solution compositions different from their own stoichiometric composition. Incongruent dissolution of a double salt is accompanied by the formation of a secondary solid phase, i.e. one of the pure single salts that form the double compound crystallizes out. In this respect, the behavior of double salts during wetting is similar to that of other salts, e.g. anhydrous Na_2SO_4 (thenardite), that form metastable solutions, i.e. solutions supersaturated with respect to other solids (e.g. $Na_2SO_4 \cdot 10H_2O$, mirabilite). Consequently, double salts may have a great damage potential because a solution supersaturated with respect to one of the single salt compounds is formed during their dissolution. Therefore, crystallization and damage may occur at high relative humidity (deliquescence of the double salt) or during wetting. Recently, this behavior was confirmed in wetting experiments with thenardite and darapskite by in situ Raman spectroscopy [14]. During wetting of both thenardite and darapskite we observed the formation of mirabilite. In the present study, similar wetting−drying experiments were carried out with an equimolar salt mixture Na_2SO_4–$MgSO_4$. In situ Raman microscopy was used to study the phase transformations during wetting.

2   Materials and methods

2.1   Syntheses of double salts

As discussed in more detail in Section 3.1, the only stable phases in the ternary system Na$_2$SO$_4$–MgSO$_4$ at 23 °C are epsomite (MgSO$_4$·7H$_2$O), mirabilite and bloedite. However, initial experiments on evaporation of equimolar solutions revealed that a second double salt, konyaite, formed next to bloedite depending on the climatic conditions during evaporation. Pure bloedite was prepared by addition of NaCl to a MgSO$_4$ solution at 40 °C and cooling to room temperature as described in reference [15]. The identity of the product was confirmed by XRD (PDF 19-1215) and a sample was used to record the Raman spectrum. Evaporation of an equi-molar mixed solution at room temperature yielded two different types of crystals that could be separated using tweezers. The two solids were iden-tified by XRD as thenardite (PDF 37-1465) and konyaite (PDF 35-0649). Thenardite was also identified via Raman spectroscopy using the refe-rence spectrum reported earlier [13]. The konyaite crystals were used to determine the Raman spectrum of the double salt.

For the preparation of the bloedite crystals used in the wetting experi-ments, an equimolar mixed solution was prepared by dissolving 23.76 g (0.167 mol) Na$_2$SO$_4$ and 38.5 g (0.168 mol) MgSO$_4$·6H$_2$O in 142.1 g doub-ly distilled water. Few milliliters were filled in Petri dishes and evaporated in a desiccator over a saturated solution of Ca(NO$_3$)$_2$·4H$_2$O (50% RH) at room temperature. After 51 days, pure bloedite crystals were obtained and identified via Raman spectroscopy.

The synthesis of konyaite crystals followed the same way as for bloedite. The amount of salts used were 123.3 g (0.868 mol) Na$_2$SO$_4$ and 198.3 g (0.867 mol) MgSO$_4$·6H$_2$O dissolved in 1406 g double distilled water. As desiccant, a saturated solution of K$_2$CO$_3$·1.5H$_2$O generating a relative humidity of about 43%, was used. After a few days, pure konyaite crystals were obtained and identified via Raman spectroscopy.

2.2   Wetting experiments and in situ Raman observations

The in situ Raman observations during wetting of salt crystals were per-formed on glass slides which were cleaned with hydrogen peroxide to remove all organic substances. Experiments were done with pure crystals of bloedite and konyaite. In situ observations started with the recording of the Raman spectrum of the pure educt phases. Subsequently, the sample was carefully wetted with 2–4 µL of doubly distilled water using a microliter pipet. The amount of water used was chosen in order to avoid complete dissolution and the formation of a dilute undersaturated solution. In this

case, no information on the precipitation of a new phase is obtained and the subsequent drying will be similar to a droplet evaporation experiment. Right after the addition of water Raman spectra were continuously recorded at the same spot of the sample surface. Occasionally, the crystal under investigation changed its position slightly due to the presence of the solution. In these cases, the laser was adjusted accordingly.

2.3   Instrumentation

Raman spectra were recorded on a Senterra Raman dispersive microscope (Bruker Optics GmbH, Germany) with an automated Raman frequency calibration system (SurCal technology) using MPlan M 10x and LMPlanFL N 20x objectives (Olympus Deutschland GmbH, Germany). The diode-laser excitation source was operated at 532 nm and 20 mW.

The Raman spectrum of a mixture of different solid phases can be expressed as the linear combination of the spectra of the pure compounds:

$$I(\lambda) = \sum_i \left(b_i \, I_{r,i}(\lambda) \right) \tag{1}$$

where $I(\lambda)$ is the intensity at wavelength λ (the observed Raman spectrum) and $I_{r,i}(\lambda)$ are the spectra of the reference compounds r. The coefficients b_i can be determined by multiple linear regression and ordinary least squares analysis using reference spectra of all compounds that might be present in the mixture under investigation. Details on the measurements of the reference spectra are provided in reference [13]. The least squares analysis was carried out using a selected number of wavenumbers at which the measured intensities in both the sample and the reference spectra were sufficiently high. The coefficients b_i represent the contributions of the reference spectra to the sample spectrum. No attempts were made to calibrate the method, i.e. the values of b_i do not represent but are related to the mole fractions of a compound.

3   Results and discussion

3.1   Solubilities in the ternary system Na_2SO_4–$MgSO_4$–H_2O

There is a number of solid phases that may be formed in the ternary system Na_2SO_4–$MgSO_4$–H_2O [16]. These are listed in Table 1. Nine of these phases do have ranges of stable existence, only six phases (thenardite, mirabilite, kieserite, hexahydrite, epsomite and bloedite) can be stable at near ambient temperatures, meaning that these solids have lower solubili-

Table 1: Possible phases in the ternary system of Na$_2$SO$_4$–MgSO$_4$–H$_2$O

Compound	Formula	Thermodynamics
thenardite (phase V)	Na$_2$SO$_4$ (V)	stable[a]
phase III	Na$_2$SO$_4$ (III)	metastable
sodium sulfate heptahydrate	Na$_2$SO$_4$·7H$_2$O	metastable
mirabilite	Na$_2$SO$_4$·10H$_2$O	stable[a]
kieserite	MgSO$_4$·H$_2$O	stable[a]
magnesium sulfate 5/4 hydrate	MgSO$_4$·1.25H$_2$O	metastable
sanderite	MgSO$_4$·2H$_2$O	metastable
magnesium sulfate trihydrate	MgSO$_4$·3H$_2$O	metastable
starkeyite	MgSO$_4$·4H$_2$O	metastable
pentahydrite	MgSO$_4$·5H$_2$O	metastable
hexahydrite	MgSO$_4$·6H$_2$O	stable[a]
epsomite	MgSO$_4$·7H$_2$O	stable[a]
meridianiite	MgSO$_4$·11H$_2$O	stable[b]
bloedite	Na$_2$Mg(SO$_4$)$_2$·4H$_2$O	stable[a]
konyaite	Na$_2$Mg(SO$_4$)$_2$·5H$_2$O	metastable
loweite	Na$_{12}$Mg$_7$(SO$_4$)$_{13}$·15H$_2$O	stable[c]
vanthoffite	Na$_6$Mg(SO$_4$)$_4$	stable[c]
disodium magnesium sulfate decahydrate	Na$_2$Mg(SO$_4$)$_2$·10H$_2$O	metastable

[a] stable at near ambient temperatures
[b] stable at low temperatures (<0.7 °C)
[c] stable at enhanced temperature (loeweite: >57 °C, vanthoffite: >60 °C)

ties (for a given mixture composition) than the metastable phases which have higher saturation concentrations. However, due to the tendency of several stable solids to supersaturate, the saturation concentrations of various metastable solids can be reached and exceeded during evaporation. Mirabilite and kieserite exhibit a particularly strong tendency to supersaturate. Therefore, the formation of metastable sodium [4,17] and magnesium sulfate phases [16] is quite commonly observed.

The solubility diagram of the Na$_2$SO$_4$–MgSO$_4$-system at 23 °C is shown in Figure 1. The solubilities were calculated using our thermodynamic model [16,18] and validated with available experimental data [16]. There are three thermodynamically stable phases: mirabilite, bloedite and epsomite. Their solubilities are represented by the solid black lines. The dashed lines represent the solubilities of the metastable phases thenardite, phase III, heptahydrate, hexahydrite, starkeyite, kieserite and the metastable branch of the bloedite solubility curve. The solid grey line indicates an equimolar mixed solution of both salts. During evaporation the solution will first reach
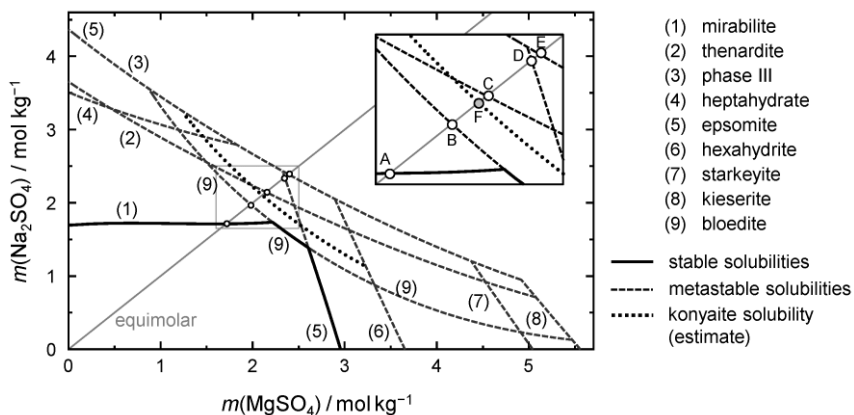
Figure 1: Solubility diagram of the system Na_2SO_4–$MgSO_4$–H_2O at 23 °C calculated using an equilibrium model [16,18]. Solid and dashed curves denote stable and metastable solubilities, respectively. The gray solid line represents an equimolar mixed solution. Points A, B, C, D, E and F represent saturation concentrations in the equimolar solution with mirabilite, bloedite, thenardite, epsomite, phase III and konyaite, respectively. The dotted curve represents estimated solubilities of konyaite.

saturation with the stable solid mirabilite (at point A) confirming that bloedite is incongruently soluble.

In our evaporation experiments with an equimolar mixed solution the formation of mirabilite was not observed due to its strong tendency to supersaturate. Upon further evaporation into the supersaturated region the concentration increases and reaches successively saturation with bloedite, thenardite, epsomite and phase III (points B–E). An enlarged view is provided in the inset of Figure 1. It can be understood that bloedite is formed in our evaporation experiments with an equimolar mixed solution. If the evaporation rates are not too large (at about 50% RH), the critical concentrations for thenardite and phase III nucleation are obviously not reached. However, increasing the evaporation rate by slightly decreasing the RH in the desiccator results in higher supersaturation and crystallization of konyaite. In some experiments the simultaneous crystallization of konyaite and thenardite was also observed.

Unfortunately, the available thermodynamic data for konyaite do not permit the calculation of its solubility. However, it is certain that konyaite is metastable with respect to bloedite and, most likely, will have a solubility close to that of thenardite at 23 °C. Based on these assumptions we have

drawn an estimated solubility curve for konyaite in Figure 1 (dotted line). Saturation with konyaite is indicated by point F.

3.2   Raman reference spectra

The use of Raman microscopy for the in situ analysis of phase transformations in the wetting experiments requires Raman reference spectra of all possible phases. Phase identification is possible by comparison of the position of the total symmetric stretching vibration (ν_1) of the sulfate ion. The reference spectra with the spectral range dominated by the ν_1 Raman peak positions of the compounds relevant to this work are depicted in Figure 2. There is a systematic shift of the ν_1 peak position that can be used for phase identification. In cases when the difference in the ν_1 peak position is only small, additional information may be gained from less intense Raman bands (not shown in Figure 2).

Usually, it is possible to identify unambiguously the different phases present in a mixture. In case of a very complex mixture composition, additional information, e.g. from phase diagrams, can be used to assess the
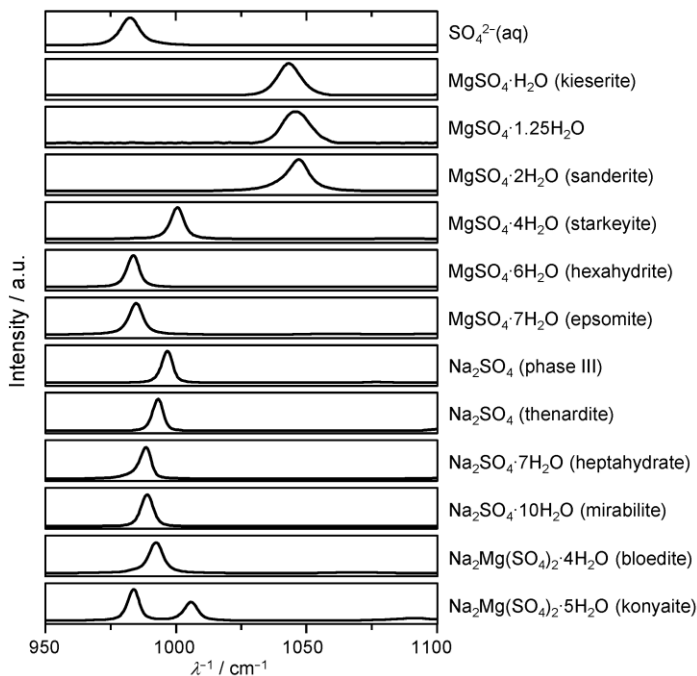
Figure 2:   Raman reference spectra in the spectral range dominated by the symmetric stretching vibration of the SO_4 tetrahedra (950 cm^{-1} and 1100 cm^{-1}).

most likely phase assemblages. However, it is always very difficult to distinguish epsomite and hexahydrite unambiguously.

3.3 In situ Raman observations during wetting

3.3.1 Wetting of pure konyaite crystals

The results of the in situ Raman measurements during the wetting of pure konyaite are shown in Figure 3. The spectrum on top of the left diagram was recorded right before the addition of water and confirms the presence of pure konyaite with two characteristic peaks assigned to the symmetric stretch of sulfate. The two peaks correspond to two distinct sulfate tetrahedra in the structure of konyaite [19]. Only one of them is coordinated directly to the Mg^{2+} ion. The second spectrum (0 min) was recorded right after the addition of water. The konyaite peaks no longer occur in the spectrum and the peak assigned to the aqueous sulfate ion appears instead. At that moment in time, the sample was not yet completely dissolved. However, the laser was focused on a spot in the center of the droplet where the dissolution was already complete. At the edge of the droplet (not shown in the respective micrograph) there was still a solid residue of konyaite.

After about 11 min the re-appearance of the peak at 1005 cm^{-1} indicates the precipitation of konyaite during evaporation of the droplet. In the following spectra the peak caused by SO_4^{2-}(aq) continuously diminishes while the konyaite peaks increase indicating ongoing evaporation and precipitation of konyaite. Assuming that konyaite is the only solid phase present we calculated by least squares analysis the contributions of dissolved sulfate and crystalline konyaite to the various spectra. The result of these calculations is depicted in Figure 3 (right diagram) and yields an approximate composition after wetting and during evaporation. Although konyaite is an incongruently soluble salt its behavior in the wetting and drying experiment is that of a congruently soluble salt, i.e. it dissolves without precipitation of a second salt (which would be mirabilite in this case) and is re-precipitated during evaporation.

From the Raman spectra it may be speculated that hexahydrite or epsomite might have been formed as well. However, this is very unlikely as these salts exhibit much higher solubilities than bloedite, konyaite and thenardite (cf. Figure 1). Also, if a magnesium sulfate hydrate would have been formed, for stoichiometric reasons, a sodium sulfate phase would have to be formed as well which is clearly not the case. Finally, it is surprising that the calculations predict the presence of a solution still after 28 min (cf. Figure 3). It is not clear whether this is an indication that there is
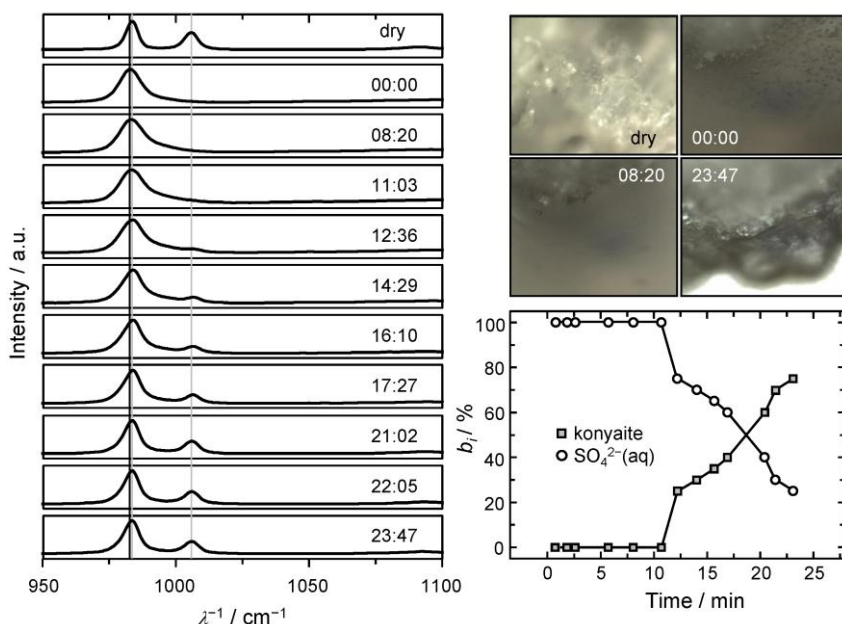
Figure 3: In situ Raman microscopy after wetting of konyaite. Left diagram: initial Raman spectrum of dry konyaite sample and successively recorded spectra after wetting; the vertical lines represent the peak positions in the reference spectra of konyaite (grey) and of an aqueous sulfate solution (black). The micrographs show the sample before and at different times after wetting. Lower right diagram: approximate composition of the sample during wetting (represented by the coefficients b_i of Eq. 1).

really solution left at the end of the measurements and the resolution of micrographs is not sufficient to identify the presence of a solution with certainty. However, additional Raman spectra were recorded after several days. Only konyaite could be identified in the spectra of this completely dried sample.

3.3.2 Wetting of pure bloedite crystals

The interpretation of the wetting experiment with bloedite crystals turned out to be more complicated. The results are shown in Figure 4. The first spectrum confirms bloedite as the starting material which is dissolved completely after the addition of water (second spectrum in Figure 4). During the following 40 min a precipitate forming a thin layer on top of the solution droplet started to grow (see micrographs after 18 and 41 min). Upon closer inspection of the Raman spectra a slight shift of the peak maximum can be seen and also a decrease in the peak width. This is a
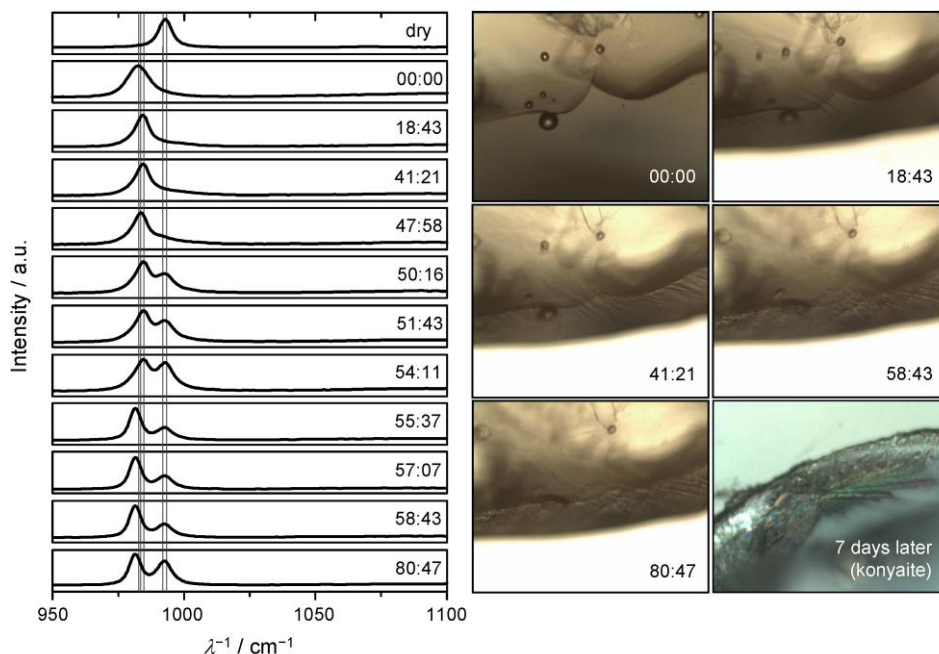
Figure 4: In situ Raman microscopy after wetting of bloedite. Left diagram: initial Raman spectrum of dry bloedite sample and successively recorded spectra after wetting; the vertical lines represent the peak positions in the reference spectra of aqueous sulfate, hexahydrite, epsomite, bloedite and thenardite (from left to right). The micrographs show the sample before and at different times after wetting.

clear indication for the presence of either hexahydrite or epsomite as the main constituent of the crystalline layer. This is in agreement with the observation of such layers in droplet evaporation experiments with pure $MgSO_4$ solutions. In these experiments the crystalline layers hindered further evaporation of the droplet and made it extremely difficult to detect other crystalline phases or aqueous solutions that are present underneath.

There is no significant change in the Raman spectra during the first 50 min after the addition of water although the micrographs clearly show the continuous growth of the layer. Only then, a second peak at about 993 cm^{-1} occurred in the spectrum (50 min). This peak may be assigned to thenardite, however, the peak position is also close to the peak in the reference spectrum of bloedite (992.3 cm^{-1}) and it is impossible to ascribe this peak to either one of these two solids with certainty. Due to the uncertainties regarding the identity of the solid phases no calculations of the sample compositions were carried out.

In the following 30 min the spectra do not alter very much apart from changes in the intensity ratios of the two peaks that may be caused by minor movements of solution and crystalline deposits during evaporation resulting in a small displacement of the laser spot. According to the micrographs, solution is still present after 80 min, therefore, the last spectrum probably represents a mixture of dissolved sulfate, epsomite (or hexahydrite) and either thenardite or bloedite.

After 7 days of drying several Raman spectra of the completely dry sample were recorded. Surprisingly, konyaite was found as the main constituent with minor contributions of a second phase (thenardite or bloedite). Since it is unlikely that konyaite is formed by conversion from bloedite (usually the opposite is observed [19]), we conclude that a likely crystallization pathway after wetting includes the initial formation of epsomite (or hexahydrite) followed by thenardite precipitation and, subsequently, with ongoing evaporation the formation of konyaite. Considering the solubility diagram (Figure 1), the crystallization of epsomite (or hexahydrite) is surprising as this requires very high supersaturation with respect to bloedite, konyaite and thenardite. However, if it is accepted that a magnesium sulfate hydrate crystallizes first (epsomite being more likely), the remaining solution becomes enriched in sodium sulfate. It can then be understood that thenardite is the second solid phase that is precipitated as the solution is no longer equimolar (cf. Figure 1). In contrast to the wetting experiment with konyaite, this compound did not crystallize as the first solid in the wetting experiment with bloedite. One reason may simply be that nuclei acting as seed crystals were still present after the initial dissolution of konyaite.

In conclusion, also bloedite does not follow the expected behavior of an incongruently soluble salt upon wetting. For incongruent dissolution the precipitation of mirabilite is expected (cf. Figure 1). Obviously, the supersaturation with respect to mirabilite in a solution saturated with bloedite is not sufficient for the nucleation of mirabilite. Crystallization only occurs after further increase of the solution concentration during evaporation. Under these conditions other phases than mirabilite are formed.

3.3.3 Comparison to single salt behavior and damage potential

Sodium sulfate is considered as one of the most damaging salts in building materials and is frequently used in laboratory crystallization tests. It is well known that the destructive process is the growth of mirabilite crystals from the highly supersaturated solutions originating from the dissolution of anhydrous Na_2SO_4 [4,20]. Recently, we have confirmed this reaction pathway by in situ Raman microscopy [14]. In that study we carried out wetting experiments with thenardite similar to the experiments with bloedite and

konyaite in the present work. Wetting of thenardite with a limited amount of water leads to the formation of a solution saturated with thenardite. At 23 °C, the temperature of the wetting experiments, the solubility of thenardite is more than twice that of mirabilite. Hence, mirabilite crystallization occurs under conditions of very high supersaturation resulting in substantial crystallization pressure [4].

Similar behavior is expected in the case of magnesium sulfate. However, the resulting supersaturation depends on the nature of the lower hydrated phase, i.e. on the degree of dehydration after drying. Very high supersaturation resulting in significant stress is generated during the wetting of the lowest hydrate of magnesium sulfate, i.e. $MgSO_4 \cdot H_2O$ (kieserite) [7,8].

Similar behavior was also demonstrated in wetting experiments with the incongruently soluble double salt $Na_3NO_3SO_4 \cdot H_2O$ (darapskite). After wetting of darapskite rapid crystallization of mirabilite from a substantially supersaturated solution was observed by Raman microscopy [14]. In the wetting experiments carried out in the present work, the supersaturation with respect to mirabilite of a solution just saturated with bloedite is only about 15%. This is obviously not enough for nucleation to occur in our experiment. However, even if nucleation occurred, the resulting crystallization pressure is expected to be low at such moderate supersaturation. Assuming that the supersaturation of 15% can be maintained during crystal growth, a maximum crystallization pressure of only 2.2 MPa is calculated at 23 °C. This value is significantly lower than the values of 12.3 MPa and 10.6 MPa that are obtained for the wetting of thenardite and phase III, respectively, at the same temperature, thus indicating that the damage potential of the dissolution of the incongruently soluble double salt bloedite is much lower. Also in comparison to the wetting of darapskite, which yields a crystallization pressure of 4.4 MPa at the same temperature, the damage potential of bloedite appears to be lower. This is also confirmed by our ongoing wetting-drying experiments with sandstone specimens contaminated with an equimolar Na_2SO_4–$MgSO_4$ mixture. The results of these experiments will be reported elsewhere.

4   Conclusions and outlook

The dissolution of thenardite and lower hydrated phases of magnesium sulfate leads to highly supersaturated solutions. In effect, the respective higher hydrated phases, i.e. mirabilite and epsomite or hexahydrite, crystallize out. If crystal growth occurs in confinement, a high crystallization pressure can be generated. In theory, the same mechanism also applies to incongruently soluble double salts. Their dissolution leads to a solution that is supersaturated with respect to one of the single salt compounds.

Depending on the degree of supersaturation, wetting of an incongruently soluble double salt in a porous material may also cause high crystallization pressures. This mechanism was confirmed in a recent study with darapskite; its dissolution was followed by crystallization of mirabilite. In contrast, the wetting experiments carried out in the present work show that the dissolution of these salts does not lead to the expected crystallization of mirabilite. Obviously, the degree of supersaturation is not sufficient for mirabilite nucleation in our experiment. The calculation of crystallization pressures confirms that bloedite and, most likely, also konyaite are less damaging than both their single compounds, i.e. sodium sulfate and magnesium sulfate, and in comparison to darapskite, another incongruently soluble double salt.

Acknowledgement

References

[1]   Tsui N., Flatt R.J., Scherer G.W. Crystallization damage by sodium sulfate. J. Cult. Heritage 4 (2003) 109–115.

[2]   Espinosa Marzal R.M., Scherer G.W. Crystallization of sodium sulfate salts in limestone. Environ. Geol. 56 (2008) 605–621.

[3]   Angeli M., Bigas J.-P., Benavente D., Menéndez B., Ronan H., David C. Salt crystallization in pores: quantification and estimation of damage. Environ. Geol. 52 (2007) 205–213.

[4]   Steiger M., Asmussen S. Crystallization of sodium sulfate phases in porous materials: The phase diagram Na_2SO_4–H_2O and the generation of stress. Geochim. Cosmochim. Acta 72 (2008) 4291–4306.

[5]   Schiro M., Ruiz-Agudo E., Rodriguez-Navarro C. Damage mechanisms of porous materials due to in-pore salt crystallization. Phys. Rev. Lett. 109 (2012) 265503.

[6]   Desarnaud J., Bertrand F., Shahidzadeh N. Impact of the kinetics of salt crystallization on stone damage during rewetting/drying and humidity cycling. J. Appl. Mech. 80 (2013) 020911.

[7]   Steiger M., Linnow K., Juling H., Gülker G., El Jarad A., Brüggerhoff S., Kirchner D. Hydration of $MgSO_4 \cdot H_2O$ and generation of stress in porous materials. Cryst. Growth Des. 8 (2008) 336–343.

[8] Balboni E., Espinosa-Marzal R.M., Doehne E., Scherer G.W. Can drying and re-wetting of magnesium sulfate salts lead to damage of stone? Environ Earth Sci, 63 (2011) 1463–1473.

[9] Cardell C., Benavente D., Rodríguez Gordillo J. Weathering of limestone building material by mixed sulfate solutions. Characterization of stone microstructure, reaction products and decay forms. Mater. Charact. 59 (2008) 1371–1385.

[10] De Clercq H. Behaviour of limestone contaminated with binary mixtures of sodium sulphate and treated with a water repellent. Int. J. Restor. Build. Monum. 14 (2008) 357–364.

[11] Steiger M., Charola A.E., Sterflinger K. Weathering and deterioration. In: Siegesmund S., Snethlage R. (eds.) Stone in architecture, Springer, Berlin (2011) pp. 227–316.

[12] De Clercq H., Jovanović M., Linnow K., Steiger M. Performance of limestone laden with Na_2SO_4–$NaNO_3$ and Na_2SO_4–K_2SO_4 mixtures. Environ. Earth Sci. 69 (2013) 1751–1761.

[13] Linnow K., Steiger M., Lemster C., De Clercq H., Jovanović M. In-situ Raman observation of the crystallization in $NaNO_3$–Na_2SO_4–H_2O solution droplets. Environ. Earth Sci. 69 (2013) 1609-1620.

[14] Lindström N., Heitmann N., Linnow K., Steiger M. Crystallization behavior of $NaNO_3$–Na_2SO_4 salt mixtures in sandstone and comparison to single salt behavior. 12th International Conference on the Deterioration and Conservation of Stone. New York, 2012.

[15] Autenrieth H., Braune G. Die Lösungsgleichgewichte des reziproken Salzpaares Na_2Cl_2+$MgSO_4$+H_2O bei Sättigung an NaCl unter besonderer Berücksichtigung des metastabilen Bereichs. Kali Steinsalz 3 (1960) 15–30.

[16] Steiger M., Linnow K., Ehrhardt D., Rohde M. Decomposition reactions of magnesium sulfate hydrates and phase equilibria in the $MgSO_4$–H_2O and Na^+–Mg^{2+}–Cl^-–SO_4^{2-}–H_2O systems with implications for Mars. Geochim. Cosmochim. Acta 75 (2011) 3600–3626.

[17] Hamilton A., Hall C, Pel L. Sodium sulfate heptahydrate: direct observation of crystallization in a porous material. J. Phys. D 41 (2008) 212002-1/5.

[18] Steiger M., Kiekbusch J., Nicolai A. An improved model incorporating Pitzer's equations for calculation of thermodynamic properties of pore solutions implemented into an efficient program code. Construct. Build. Mater. 22 (2008) 1841–1850.

[19] Leduc E.M.S., Peterson R.C., Wang R. The crystal structure and hydrogen bonding of synthetic konyaite, Na$_2$Mg(SO$_4$)$_2$.5H$_2$O. Am. Mineral. 94 (2009) 1005–1011.

[20] Flatt R.J. Salt damage in porous materials: how high supersaturations are generated. J. Cryst. Growth 242 (2002) 435–454.